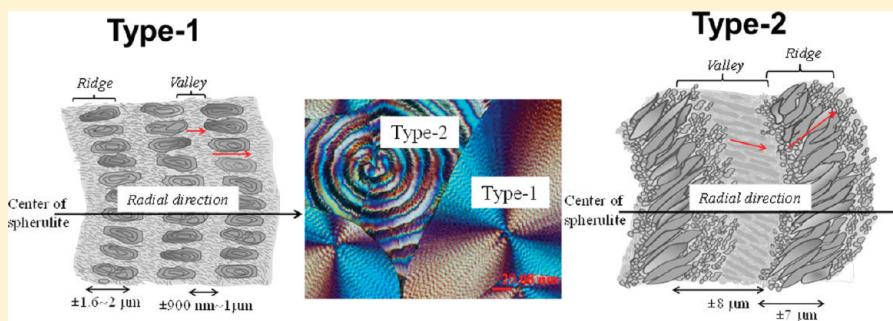


Surface Nanopatterns of Two Types of Banded Spherulites in Poly(nonamethylene terephthalate) Thin Films

E. M. Woo* and Siti Nurkhamidah

Department of Chemical Engineering, National Cheng Kung University, Tainan, 701, Taiwan



ABSTRACT: Surface nanopatterns of dual ring-banded spherulites in poly(nonamethylene terephthalate) (PNT) were investigated using polarized optical microscopy (POM) and atomic force microscopy (AFM). The surface morphology differs between narrow-spaced single ring bands versus widely spaced double ring bands in spherulites, labeled Type-1 and Type-2, respectively. Ridge and valley consist of two discrete species ranging from nano- to micrometer-sized crystals shaped and oriented differently. Ridges of Type-1 and Type-2 spherulites apparently differ in shapes of the crystal plates. AFM height profile analysis reveals that the ridge of Type-2 ring-banded spherulite is higher than that of Type-1 spherulites. The crystal packing on the ridges and valley of these two types of ring-banded was further compared using high-magnification AFM phase imaging. There exists a transition zone in going from the ridge and valley regions in the Type-2 ring-banded spherulites crystallized at $T_c = 75\text{--}85^\circ\text{C}$; the crystals on the transition zone change gradually in sizes and orientation from those in the ridge to valley. By contrast, Type-1 ring-banded spherulite does not have this kind of transition zone, meaning that crystals in the ridges abruptly submerge into valley in Type-1 ring-banded spherulites. Details of packing of nanosize crystals in forming ridge and valleys of these two ring band types are discussed.

1. INTRODUCTION

Two types of ring-banded spherulites (single- and double-ring-banded, respectively) coexisting in poly(nonamethylene terephthalate) (PNT) crystallized at a T_c have been earlier reported.^{1,2} Dual types of ring-band patterns in spherulites are known to exist in PNT cast as thin films crystallized at a given temperature. PNT has been proven to be the only one or one of very few polymers capable of simultaneously showing two types of ring-banded spherulites at the same T_c , whose relative percentages of each type vary depending on the crystallization temperature as well as external nuclei.¹ PNT exhibiting two types of ring-banded spherulites has been characterized on surface and interior 3-D using SEM^{1,2} and AFM techniques.² It has been shown that, in addition to the fact that the inter-ring spacing of Type-2 spherulite is greater than that of Type-1 spherulite in PNT, AFM height profile analysis reveals that the ridge of Type-2 ring-banded spherulites is higher than that of Type-1 spherulites.² Ring-banded spherulites in some semicrystalline polymers may be common and widely reported; however, the coexistence of two or more types of ring-banded spherulites in the same polymer is rare. The two types of ring bands differ significantly on the birefringence, inter-ring spacing, and surface and inner lamellar assembly.

Periodic banding mechanisms have remained controversial since long ago, although many investigators have attempted to search universal interpretations. Two basic proposals for mechanisms of twisting are more often cited: (I) lamellar twisting with features that generate during the growth process,^{3,4} and (II) lamellar twisting with features that are associated with lamellae themselves, such as screw dislocations^{5,6} or surface stress at fold faces.⁷ However, such concept of stresses may experience difficulty in universality, as not all polymers show ring-banded spherulites. In addition to such complexity, the patterns of ring bands in different polymers can also differ significantly; and the ring band patterns of the same polymer can differ significantly by crystallization at a different temperature. Murayama⁸ has earlier reported so-called double-rings (bands of a wide interspacing and of two alternating colors) in poly(ethylene adipate) (PEA) and proposed a few models based on the mechanism of lamellar twisting; however, the POM optical properties of these double rings were determined to be not yet fully fitted with the supposed twisting

Received: February 3, 2012

Revised: March 28, 2012

Published: April 5, 2012



models. Overall, the issues remain controversial with ongoing debates.

AFM has been widely applied to investigate surface topography, lamellar, and crystal structures including banded rings in spherulites,^{9–13} or shish-kebab dendrites in ultrathin-film polyethylene, etc.¹⁴ To utilize the free-surface nature of AFM in dealing with the difficulty and complexity in the subject of ring-banded crystals in polymers, more innovative procedures were needed. A twisting lamella has been proposed by many as a plausible mechanism in interpreting ring bands in polymers, such as poly(vinylidene fluoride) (PVF₂) spherulite systems by Briber and Khouri,¹⁵ who dealt with semibulk-form (20 μm for SEM, etc.) of a PVF₂/PVA blend, in which experimental procedures involved sample treatments with solvent such as acetone, DMF, etc., for TEM or SEM characterizations. Lamellar twisting, like chain folding, is not thermodynamically the most stable form, and crystals packed into ring-bands in spherulites may yet assume several forms depending on kinetics (such as temperature, supercooling, diffusion limitation due to geometrical forms/thickness, etc.). Thus, correlations between the lamellae twisting and ring bands may be questioned again. In such cases, whether or not twisting in lamella seen in the interior of a bulk can be correlated to the ring-banded morphology was restricted to the outer surface of the bulk. These observations mean that twisting lamellae may not explain the ring bands, at least for PBA, due to the fact that if twisting lamellae were responsible for bands, then ring bands should also have been present in interiors or underside of the bulk, as well as on the outer surface. In the investigation on ring bands in poly(3-hydroxybutyrate-*co*-3-hydroxyhexanoate) (PHB-*co*-HH), Xu et al.¹⁶ claim that twisting of lamellae can be seen only in the early stage of crystallization, while after the lamellae were filled, twisting cannot be seen any more, and Xu et al.'s work has shown a lamella twist with dimension of ~0.5–1 μm in length, assuming grass-leaf geometry, sparsely grown, at early stage of 75 °C. They claimed a correlation between the ring bands in P(HB-*co*-HH) spherulites fully grown at 45 °C to the early stage twist of lamellae grown at 75 °C. Questions arise again in attempting to establish such a correlation. The ring-bands grown at 45 °C in PHB copolymer are multiple rings up to 10 periods with spacing of 1–2 μm, but the ring band period (inter-ring distance) for PHB copolymer at higher temperatures can even be as large as 3–5 μm. On the other hand, for PHB, the twist as shown is a single turn in the early stage lamella formed at 75 °C, with a twist spacing of about 0.3–0.5 μm. As such, a single twist of 0.3–0.5 μm in early stage lamellae does not seem to be adequate for explaining the multiple ring bands of 3–5 μm spacing. It will not be convincing to extrapolate that the morphology at early stage will remain the same as the fully grown crystal morphology, assuming the same shape trend but the scales expanding. Besides, there are ample classical cases where lamellar twisting is present in early stage crystals, but when fully grown, no ring bands are present in polymers such as iPP or sPS,^{17–21} or other crystalline polymers.^{22,23} Thus, twisting in lamellae, especially those near and restricted to central eyes of spherulites, cannot always be taken as correlation to ring bands that are formed at later stages and located far away from the central eyes. A single twist in a few microscopic lamellae is not readily and not necessarily correlated to the rhythmically arranged macroscopic ring bands in spherulites of 30 μm in diameters. For example, the AFM graph for a Maltese-cross (ringless) spherulite of PEA

also reveals numerous edge-on lamellae scattering among flat-on ones; however, no ring bands can be found.

AFM has been used to reveal the surface textures of the ringless versus ring-banded spherulites in poly(butylene adipate) (PBA)²⁴ and PNT,² and demonstrated that there are sufficient domain and orientation differences in the surface topography between ring-banded and ringless spherulites. In continuing with previous work on revealing the interior 3D lamellar assembly to disseminate the correlation between the surface and inner ring-banded crystal patterns in PNT, the objective of this study was to further analyze the minute details of surface patterns of the unusual dual types of ring-banded PNT spherulites by focusing on the nanosize morphology of lamellar textures and their crystal packing differences between the Type-1 and Type-2 ring bands. Most other polymers show only a single type of banding morphology; PNT by contrast shows two entirely different types of ring bands. Consequently, the surface nanopatterns of lamellar assembly in correlation with the two banding structures in PNT served as ideal models for analyzing the banding mechanisms and insights into reasons resulting in two entirely different but simultaneous coexisting ring-banded patterns in the same polymer system crystallized at the same T_c . In this study, by using the characteristically unusual dual types of ring-banded spherulites in PNT as a model, the nanoscale surface morphology in these two-banding supermolecular/lamellar structures and their respective assembly were further investigated and analyzed.

2. EXPERIMENTAL SECTION

2.1. Materials and Preparation. Poly(nonamethylene terephthalate) (PNT) was synthesized from appropriate glycol (1,9-nonenediol) and dimethyl terephthalate using 0.1% butyl titanate as catalyst via two-step polymerization, which has been disclosed in greater detail in a previous study.¹ The PNT product was purified via reprecipitation and washing at least two times. The weight-average molecular weight and polydispersity index of PNT determined by GPC (Waters, U.S.) using polystyrene as a standard were 32 700 g/mol and 1.44, respectively. PNT was preliminarily characterized using DSC (Diamond Pyris, Perkin-Elmer Corp., U.S.) to obtain $T_g = 0.1$ °C and apparent $T_m = 91.6$ °C (10 °C/min). For sample preparation, PNT was dissolved in chloroform (2–4 wt % solution). Polymer solution was deposited on a glass slide as substrate at ambient temperature to form thin films, with no top cover glass slide. When crystallized at the same T_c , the ring band patterns in PNT were found to be identical in samples with or without top cover glass. For microscopy characterization, samples were all prepared without a top cover. The cast samples were dried by vaporizing under a hood at a controlled temperature for at least 1 day. These samples were melted at $T_{\max} = 120$ °C for 2 min, and then quickly quenched to a designated temperature for isothermal crystallization $T_c = 75$ –85 °C.

2.2. Apparatus and Procedures. Polarized-light optical microscopy (POM, Nikon Optiphot-2) equipped with a charge-coupled device (CCD) digital camera and a microscopic heating stage (Linkam THMS-600 with TP-92 temperature programmer) was used for preliminary confirmation of ringless and ring-band spherulites in samples prepared by crystallizing at the procedures described in previous section.

Atomic Force Microscopy (AFM). AFM investigations were made in intermittent tapping mode of AFM (*diCaliber*, Veeco Co., Santa Barbara, CA) with a silicon-tip ($f = 70$ kHz, $r = 10$

nm). The largest scan range was $150 \mu\text{m} \times 150 \mu\text{m}$, but the smallest range could be down to $5 \mu\text{m} \times 5 \mu\text{m}$ for larger magnifications on selected areas of interest. Thin films were deposited on substrates of glass slides, with an open face for AFM characterization. The top surfaces of the film samples were exposed with no top cover glass.

3. RESULTS AND DISCUSSION

It has been widely known that some polymers may exhibit ring-banded spherulites when crystallized at a certain T_c , but PNT is probably the only known polymer that exhibits two types of banded spherulites (termed as Type-1 and Type-2) coexisting when crystallized at a T_c . The main morphology features of these two types of banded PNT spherulites, as well as their interior lamellar assembly, are known to differ widely.^{1,2} Optical microscopy could not reveal nanoscale morphology in the ring-banding lamellar assembly of two different patterns, but the optical birefringence in these two banding types could clearly show the periodical crystal orientation. OM and AFM characterizations revealed general surface features of ring-banded spherulites in PNT isothermally melt-crystallized at $T_c = 75\text{--}85^\circ\text{C}$ for 10–30 min. Figure 1 shows POM graphs of

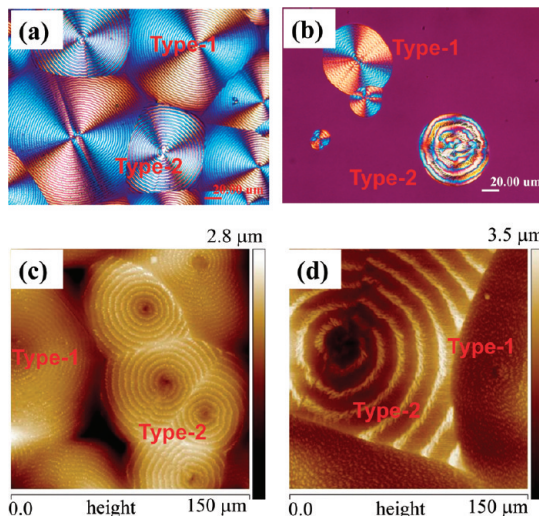


Figure 1. PNT thin films melt-crystallized: POM graphs at (a) 75, (b) 85 °C; and AFM height images at (c) 75 and (d) 85 °C.

PNT films melt-crystallized at (a) 75 and (b) 85 °C, and AFM height images of PNT films melt-crystallized at increasing T_c of (c) 75 and (d) 85 °C. The POM and AFM overview graphs of PNT spherulites of two different types can be easily compared in this figure. The POM graphs are placed on top for direct comparison to the AFM characterization. It has been reported earlier that PNT crystallized at $T_c = 60\text{--}90^\circ\text{C}$ can exhibit two different types of ring-banded spherulites, with fractions affected by T_c and substrates on which it is crystallized.^{1,2} Origins of two types of banded spherulites in PNT have been discussed in earlier papers, and will not be repeated here. The objective here is simply to point out that while POM graphs could only show the difference of inter-ring spacing but not many morphology details in these two types, AFM could further show that the ridge bands are composed of discrete protruded dots of crystal domains aligned on the ridge bands. One can easily note that the AFM characterization provides morphological details in the ring bands that cannot be revealed

by using OM or even scanning/transmission electron microscopy, which require lengthy sample preparation leading to possible alteration of original fine details. In addition, AFM graphs show that the interring-spacing in Type-2 spherulites steadily increases with T_c from 4 to 15 μm for $T_c = 75\text{--}85^\circ\text{C}$, respectively. On the other hand, the inter-ring spacing in Type-1 banded spherulites does not change much in this temperature range ($75\text{--}85^\circ\text{C}$). The inter-ring spacing in Type-1 is about 2.6–2.9 μm for $T_c = 75\text{--}85^\circ\text{C}$, respectively. Such fine details could not be easily discerned in the corresponding POM graphs placed above.

The POM graphs easily distinguish the different birefringence of Type-1 and Type-2 ring bands at all T_c 's. The POM graphs show that the ring-band patterns and inter-ring spacing apparently change with T_c ; however, the minute top-surface morphology details in the ridge and valley of Type-1 and Type-2 ring-banded spherulites were beyond resolution of optical microscopy. Thus, AFM characterization of higher magnifications ($5 \mu\text{m} \times 5 \mu\text{m}$) was performed to reveal the valley regions for either Type-1 or Type-2 spherulites, which in general differ in width, and their micromorphology also differs significantly in minute features. Magnification to nanometer scales by AFM could further show better details. In addition, height profiles were compared for ridge and valley of Type-1 versus Type-2 spherulites.

For better details, AFM zoom-in magnification on single spherulites was performed on PNT crystallized at $T_c = 75\text{--}85^\circ\text{C}$. Figure 2 shows AFM height images of greater

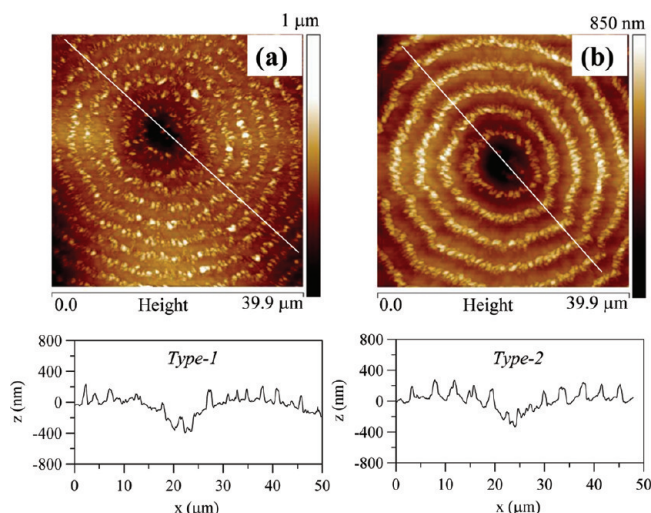


Figure 2. AFM height images of PNT films melt-crystallized at 75 °C: (a) Type-1 ring-banded spherulites and (b) Type-2 ring-banded spherulites. Height profiles along the diagonal white line are shown below each of the Type-1 and Type-2 height images, respectively.

magnifications for PNT thin-films melt-crystallized at 75 °C: (a) Type-1 ring-banded spherulites and (b) Type-2 ring-banded spherulites. Height profiles by AFM software analysis along the diagonal white line are shown below for each of the Type-1 and Type-2 height images, respectively. The vertical height (Δz) of Type-1 spherulites is about 200 nm, while that of the Type-2 spherulites is about 250 nm. Figure 3 shows similar AFM analysis ($40 \mu\text{m} \times 40 \mu\text{m}$ height images) on a PNT film sample crystallized at $T_c = 80^\circ\text{C}$. It is clear that both Type-1 and Type-2 ridge bands are composed on discrete and protruded dots (or rods) of sizes from nano- to micrometer

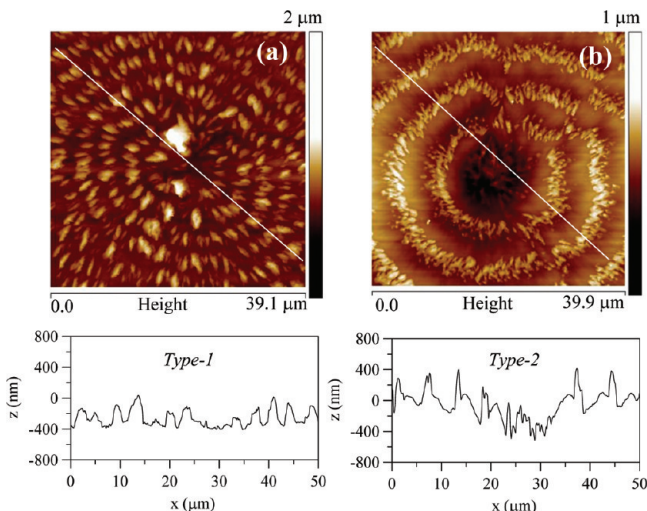


Figure 3. AFM height images of PNT films melt-crystallized at 80 °C: (a) Type-1 spherulites and (b) Type-2 spherulites. Height profiles along the diagonal white line are shown below each of the height images of Type-1 and Type-2, respectively.

scales and are aligned in different patterns to form these two banding types. These two banding types differ in several key aspects on surface patterns. First, the orientation of these rods on the ridge band is different between Type-1 and Type-2. The rods' orientation is along radial for Type-1 bands, but the orientation is at a slant angle to radial direction for the Type-2 bands. In addition, the rods are not so closely packed in Type-1 band ridge, but rods are more numerous and much more closely packed in Type-2 band ridge. Third, when crystallized at any T_c , the inter-ring spacing for Type-2 band is about twice as great as that for Type-1 band for the PNT crystallized at the same T_c . Such three features are also present in PNT crystallized at the lower $T_c = 75$ °C (previous Figure 2). The inter-ring period (pitch) for Type-1 spherulite ($T_c = 80$ °C) is ca. 3 μm; for Type-2 spherulite, the inter-ring period is about 6 μm (2 times larger than that of Type-1).

A much steeper increase in the vertical height difference with respect to T_c is seen at the higher T_c range (80–85 °C). That is, not only does the inter-ring spacing increase with T_c , but also the vertical height/drop from valley to ridge increases with T_c . Figure 4 shows AFM height images (40 μm × 40 μm) of PNT films melt-crystallized at 85 °C: (a) Type-1 ring-banded spherulites and (b) Type-2 ring-banded spherulites. Height profiles along the diagonal white line are shown below each of the height images of Type-1 and Type-2, respectively. Height profiles were also measured along the radial direction in going through the valley and ridge. Height profiles along the diagonal white line are shown below each of the height images of Type-1 and Type-2, respectively. The vertical drop Δz (height from valley to ridge) of Type-1 spherulites measured along the radial line is ±310 nm; for Type-2 spherulites, the vertical height is ±700–800 nm, which is almost 3 times as great as that for Type-1 spherulites. The inter-ring period (pitch) for Type-1 spherulite ($T_c = 85$ °C) is ca. 3 μm; for Type-2 spherulite, the inter-ring period is about 15 μm (5 times larger than that of Type-1). As shown in the POM image of Figure 1b, the width of ridge is shorter than that of valley. Thus, protruded dots of crystal domains in the transition between ridge and valley regions as indicated by arrow in Figure 4b belong to the valley region. Those discrete protrude dots go up and down in the

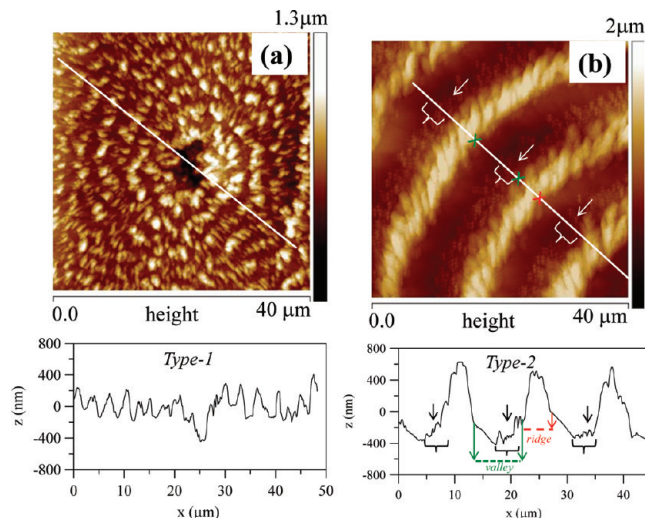


Figure 4. AFM height images of PNT films melt-crystallized at 85 °C: (a) Type-1 ring-banded spherulites and (b) Type-2 ring-banded spherulites. Height profiles along the diagonal white line are shown below of the each height images of Type-1 and Type-2, respectively.

height profile as indicated by the arrow in the height profile of Figure 4b. The detailed morphology of this transition region will be discussed later.

Height profiles were measured along the diagonal line of spherulites of both types for tracing the up-and-down of alternating ridges and valleys. For Type-1 ring-banded spherulites, the vertical height difference $\Delta z = 50$ –60 nm with every step increase of 5 °C in T_c or equivalent to ca. 10 nm for every °C increase. For Type-2 ring-banded spherulites, Δz is ca. ~200–350 nm with every step increase of 5 °C in T_c or equivalent to ca. 40–70 nm for every °C increase in T_c . With the PNT sample crystallized at even higher T_c (80–85 °C), the vertical height (Δz) difference between Type-2 and Type-1 can be as much as 2 times (450 nm vs 260 nm) for PNT sample at $T_c = 80$ °C, or 3 times for PNT sample at $T_c = 85$ °C.

The height from valley to ridge and inter-ridge spacing in Type-1 and Type-2 banded spherulites can be summarized from the above AFM analysis. Table 1 summarizes the height

Table 1. Height Difference (Δz , nm) between the Ridge and Valley Bands of PNT Films Melt-Crystallized at 75, 80, and 85 °C

type of ring-banded spherulites	crystallization temperature, T_c (°C)		
	75	80	85
Type-1	200	260	310
Type-2	250	450	800

difference (Δz) between the ridge and valley bands of PNT films melt-crystallized at 75, 80, and 85 °C. In addition, Table 2 shows that in the same spherulites, the widths of the ridge and valley are not equal, and the widths of ridge and valley vary with respect to T_c . For Type-1 ring-banded spherulites, the width of ridge is always greater than that of valley for PNT crystallized at any T_c . The valley width is 1000 nm (1.0 μm) in Type-1 ring-banded spherulites of PNT crystallized at any T_c . The ridge width in Type-1 spherulites increases with increasing T_c . For Type-2 spherulites, the opposite is true. The width of valley band is always larger than that of ridge band. For both types of ring-banded spherulites in PNT, two features are noted

Table 2. Width (μm) of Ridge and Valley Bands in Type-1 and Type-2 Ring-Banded Spherulites in PNT Thin Films Melt-Crystallized at $T_c = 75, 80$, and 85°C

type of ring-banded spherulites	crystallization temperature, T_c ($^\circ\text{C}$)		
	75	80	85
Type-1 width	ridge	1.6	1.8
	valley	1.0	1.0
Type-2 width	ridge	1.9	2.5
	valley	2.1	3.2

to change correspondingly with increasing T_c : (1) the vertical height variation from valley to ridge (Δz) increases, and (2) “protruded islands” on the ridge band become more densely spaced (for Type-1 ring-banded spherulites). For Type-1 ring-banded spherulites, the vertical height difference $\Delta z = 50\text{--}60$ nm with every step increase of 5°C in T_c , or equivalent to ca. 10 nm for every $^\circ\text{C}$ increase. For Type-2 ring-banded spherulites, $\Delta z \sim 200\text{--}350$ nm with every step increase of 5°C in T_c , or ca. 40–70 nm for every $^\circ\text{C}$ increase in T_c . A much steeper increase in the vertical height difference with respect to T_c is seen at the higher T_c range ($80\text{--}85^\circ\text{C}$).

In addition to the inter-ring periods and vertical heights, the surface morphologies of the ridge bands of Type-1 and Type-2 differ significantly. More details on the ridge band were analyzed. Figure 5 shows AFM height images and profiles along Line-1 (radial) and Line-2 (circumferential) directions, respectively, of (a) Type-1 ring-banded spherulites and (b) Type-2 ring-banded spherulites, in PNT melt-crystallized at 75°C .

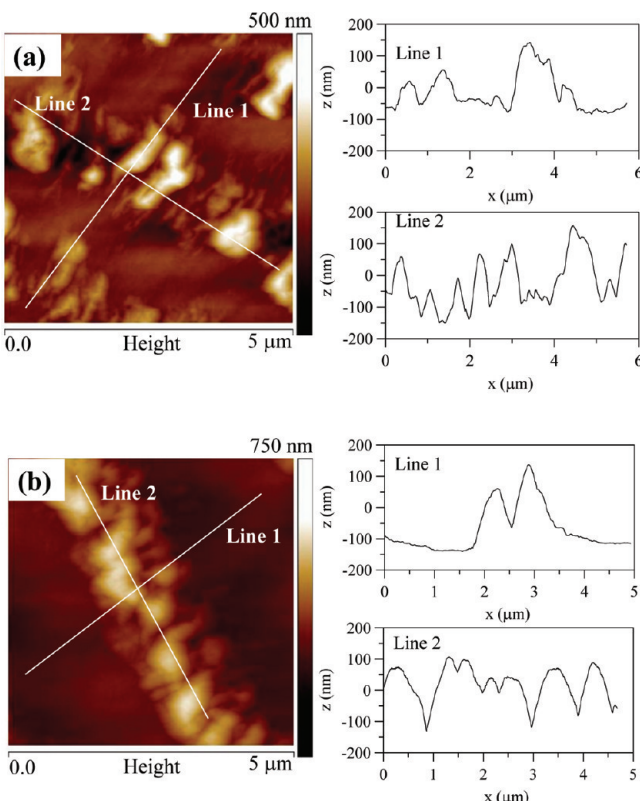


Figure 5. Zoom-in AFM height images and profiles along Line-1 (radial) and Line-2 (circumferential) directions, respectively: (a) Type-1 spherulites and (b) Type-2 spherulites, in PNT melt-crystallized at 75°C .

$^\circ\text{C}$. Line-1 is drawn along radial direction, and the up-and-down is expectedly caused by valley-ridge changes. Line-2 is along the circumferential band ridge, on which height profiles were respectively measured. That is, Line-2 does not cross the valley-ridge direction, but traverses along the ridge band. Contrary to the conventional proposal of continuous spiraling along radial, the ridge of the band is not continuous; the dot-like protrusion on the band ridge reveals an alternating up-and-down (vertical drop = 200 nm), with a rough period of ca. ~ 1 μm , suggesting that the discrete dots on the ridge have an average diameter of about 1 μm . Note, however, this up-and-down period is not in the radial direction across the ridge-valley bands, but strictly along the circumferential ridge. In addition, Figure 6 shows AFM phase images ($5 \mu\text{m} \times 5 \mu\text{m}$) for the top

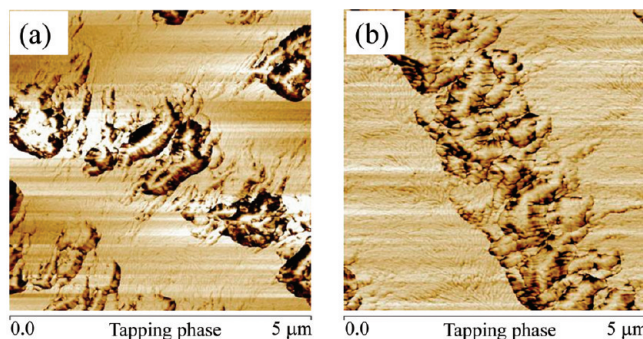


Figure 6. AFM zoom-in phase images ($5 \mu\text{m} \times 5 \mu\text{m}$) for top-surface ridge and valley of PNT films melt-crystallized at 75°C : (a) Type-1 ring-banded spherulites and (b) Type-2 ring-banded spherulites.

surface of PNT films melt-crystallized at 75°C : (a) Type-1 ring bands and (b) Type-2 ring bands on spherulite surface. The ridges of either Type-1 or Type-2 spherulites are composed of protruded lamellae aggregating as islands. When crystallized at $T_c = 75^\circ\text{C}$, the rods in Type-1 band ridge are sparsely and separately protruding out, but the rods in Type-2 band ridge are densely interconnected. The detailed morphology of the valley region in either Type-1 or Type-2 ring-banded spherulites reveals needle-like crystals in the radial direction. However, there is a transition zone between the ridge and valley regions in the Type-2 spherulites. Lamellae pattern in this region is also thin needle-like crystals; however, they are aligned in the circumferential direction instead of the radial direction.

As the rod-like crystals on the ridge bands are discrete and not continuous along the ridge, their individual height profiles could be measured along the circumferential directions. Figure 7 shows AFM height images and profiles along Line-1 (radial) and Line-2 (circumferential) directions, respectively, of (a) Type-1 ring-banded spherulites and (b) Type-2 ring-banded spherulites, in PNT melt-crystallized at 85°C . The PNT sample in this figure was crystallized at 85°C , which is 10°C higher than that in previous Figure 5. The ring band pattern remains similar, but the bandwidth and discrete dots on ridge band are increasingly greater. Similarly, AFM profiling was performed on 85°C -crystallized PNT. Line-1 is drawn along the radial direction, and Line-2 is along the circumferential band ridge, on which height profiles were respectively measured. Line-2 does not cross valley/ridge, but along the ridge band. Type-1 ring bands (Figure 7a) are compared to the Type-2 ring bands (Figure 7b) on the same PNT crystallized at 85°C . Figure 7a (along with the height profiles on right-hand-

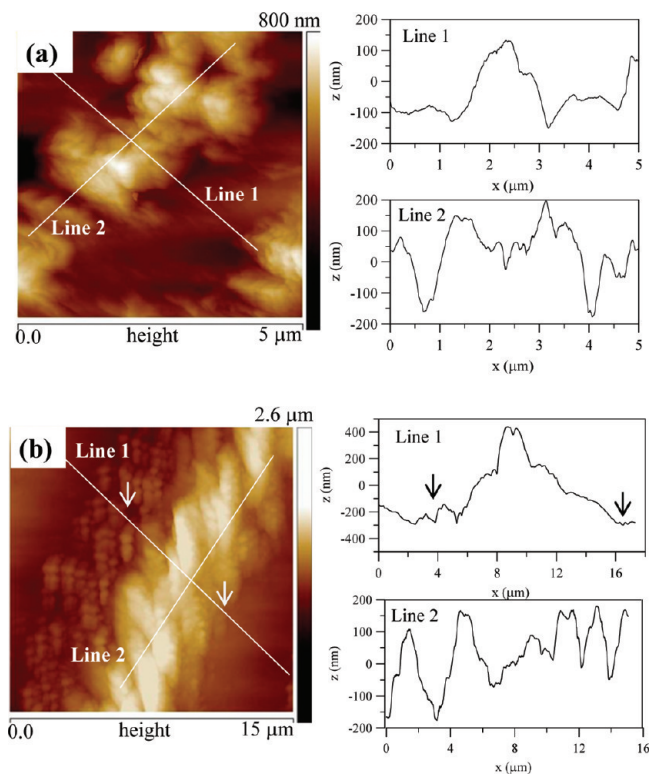


Figure 7. Zoom-in AFM height images and profiles along Line-1 (radial) and Line-2 (circumferential) directions, respectively, of (a) Type-1 ring-banded spherulites and (b) Type-2 ring-banded spherulites, in PNT melt-crystallized at 85 °C.

side) shows analyses along Line-1 and Line-2 of Type-1 banded spherulite. AFM Line-2 profile shows that the discrete dots on the ridge of Type-1 spherulite measures about 1.5 μm and have a vertical height of about 300 nm. Line-1 height profile shows that the period of valley-ridge banding is about 3 μm , and the ridge height is 300 nm, which is the same as that measured along Line-2. The similarity of vertical height as measured in Line-1 and Line-2 suggests that the dots on the ridge band are indeed discretely protruded out of the surface and they are not interconnected, but side-by-side placed on the ridge. Figure 7b (along with the height profiles on right-hand-side) shows analyses along Line-1 and Line-2 of Type-2 banded spherulite of same PNT sample crystallized at $T_c = 85$ °C. Line-1 shows that the height difference between ridge and valley is about 700 nm and the period of valley-ridge banding is about 15 μm . In the transition region between ridge and valley regions, there are discrete small protruded dots of crystal domains resulting up and down in the height profile as indicated by the arrow (left) in the height profile of Line-1 in Figure 7b. This transition region can be seen clearly in previous Figure 4b as indicated by the arrow. However, the number of discrete protruded dots of crystal domain in the transition region between valley and ridge regions is smaller than that in the transition between ridge and valley regions. Apparently, the height difference between discrete protruded dots of crystal domains in the transition region between valley and ridge regions is about 30 nm as shown by the arrow (right) in the height profile of Line-1 in Figure 7b. The detailed morphology of ridge, valley, and the transition region between valley and ridge regions or the opposite one can be seen clearly in the next figure. Type-2 bands are apparently different from the Type-1 in patterns and

banding periods, as was shown earlier in POM graphs. AFM profiling here reveals more details.

First, valley and ridge lamellae of 85 °C-crystallized Type-1 and Type-2 ring-banded spherulites were examined and compared. Figure 8 shows AFM phase images for top surface

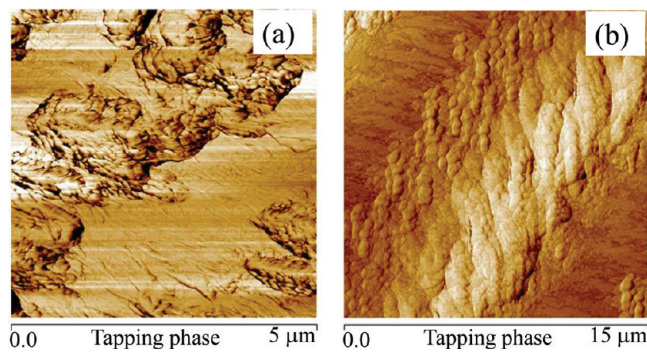


Figure 8. AFM phase images for top surface ridge and valley of PNT films melt-crystallized at 85 °C: (a) Type-1 ring-banded spherulites and (b) Type-2 ring-banded spherulites.

ridge and valley of PNT films melt-crystallized at 85 °C: (a) Type-1 ring-banded spherulites and (b) Type-2 ring-banded spherulites. The AFM phase image in Figure 8a clearly shows that the ridge band of Type-1 ring-band spherulite is composed of irregular rock-like discrete islands aligned in a circumferential pattern. The valley, by contrast, is composed of needle-like lamellae oriented roughly in radial direction. It should be noted that the morphology of lamellae in Type-1 ridges remains pretty much the same for PNT crystallized at $T_c = 70$ –85 °C in that the island-like lamellar crystals on the Type-1 ridges are discrete and irregular.

On the other hand, the crystal lamellae on ridges of Type-2 ring-banded spherulites are not discrete but are compact and jammed to each other; in addition, their patterns change significantly with increase of T_c from 75 to 85 °C. At $T_c = 85$ °C, the lamellar crystals on Type-2 ridges are shown in Figure 8b, revealing the ridges being composed of closely packed lamellar bundles, which are interwound, spiraling, and all aligned at about 45° to the radial line. That is, these lamellae on ridges are not in radial direction, but tilted at a slant angle to the radial direction. These thick lamellar bundles on the ridges then thin out thinner bundles appearing as discrete protruded dots of crystal domain before they totally merge into the valley region, and this region is called the transition region between ridge and valley. In the other side, the transition zone of valley and ridge is also composed by smaller and thinner discrete protruded dots of crystal domains. The valley region of Type-2 ring-banded spherulites is packed with very thin needle-like crystals appearing as flat-on plates oriented to roughly about 30° to the radial direction. However, lamellae in the ridge and valley of Type-2 ring-banded spherulites have different tilt directions as can be seen in Figure 8b. When lamellae in the ridge are oriented and tilted at +45°, the lamellae in the valley must be tilted at -30°.

The AFM images revealed that different lamellar assemblies of Type-1 and Type-2 ring bands collectively are reflected in their significant difference in the optical birefringence resulting from the widely different lamellar patterns and orientations. To summarize the above discussion of morphology evolution of these two different ring-banded spherulites with respect to T_c , Figure 9 shows a scheme for dotted ridge and flat valley in

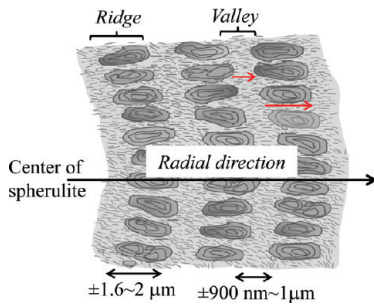


Figure 9. Scheme for dotted ridge and flat valley in Type-1 spherulites crystallized at $T_c = 70\text{--}85\text{ }^\circ\text{C}$. Lamellar directions indicated by arrows.

Type-1 spherulites of PNT crystallized at $T_c = 75\text{--}85\text{ }^\circ\text{C}$. The lamellar crystals on the ridges of Type-1 ring-banded spherulites are irregular dough-like and remain discrete (unconnected with neighboring islands), and they are aligned in circumference to form a ring. The valley region is populated with thin needle-like crystals that are aligned in radial direction. On the top surface, no gradual spiraling connection is seen between the dough-like islands (ridges) and thin need-like crystals in the valley.

The general morphology of Type-2 ring-banded spherulites changes with respect to T_c , and thus morphologies in PNT crystallized at two T_c 's are summarized for discussion. Figure 10

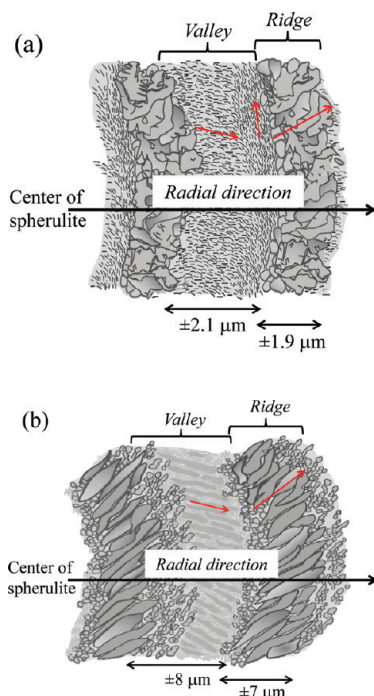


Figure 10. Schemes for AFM-analyzed morphology details in (a) Type-2 ($T_c = 70\text{--}75\text{ }^\circ\text{C}$) and (b) Type-2 ($T_c = 80\text{--}85\text{ }^\circ\text{C}$) ring-banded spherulites of PNT. Lamellar directions indicated by arrows.

shows two representative schemes for AFM-analyzed morphology details in (a) Type-2 ($T_c = 75\text{ }^\circ\text{C}$) and (b) Type-2 ($T_c = 85\text{ }^\circ\text{C}$) ring-banded spherulites of PNT. In the schemes, the radial and lamellar orientation directions are, respectively, indicated by the long and short arrows. The scheme in Figure 10a illustrates Type-2 spherulites crystallized at $T_c = 75\text{ }^\circ\text{C}$, and the scheme shows that the crystals in ridges of Type-2 spherulites are compact, overlapped, and jammed to each other, unlike the

discrete dough-like islands in ridges of Type-1 spherulites. The valley region of Type-2 spherulite at $T_c = 75\text{ }^\circ\text{C}$ is populated with thin needle-like crystals that are aligned in radial direction and are similar to the crystals in valley of Type-1 spherulites. However, there exists a transition zone between the ridge and valley in the Type-2 spherulites, and the morphology in this thin zone is also needle-like crystal, which is aligned in the circumferential direction. At higher T_c ($85\text{ }^\circ\text{C}$), the general morphology of Type-2 spherulites retains some similarity but also exhibits some distinct difference from that crystallized at lower T_c ($75\text{ }^\circ\text{C}$). The scheme in Figure 10b illustrates the Type-2 spherulites crystallized at $T_c = 85\text{ }^\circ\text{C}$, and the crystals in ridges of Type-2 spherulites are compact, overlapped, and jammed to each other; in addition, they are elongated to a longer lenticular-shape and oriented to $+45^\circ$ to the radial direction. The valley region of Type-2 spherulite at $T_c = 85\text{ }^\circ\text{C}$ is populated with thin needle-like crystals that are aligned in -30° from radial direction, and again these are similar to the crystals in valley of Type-1 spherulites. The transition region between ridge and valley or the opposite ones can be distinguished clearly from the crystal pattern on those regions. Both of these transition regions are composed by the small size of the protruded dots of the crystal domain, which is different in thickness.

Figure 11 shows (a) POM graphs of PNT films melt-crystallized at $85\text{ }^\circ\text{C}$, and (b) schemes for the optical

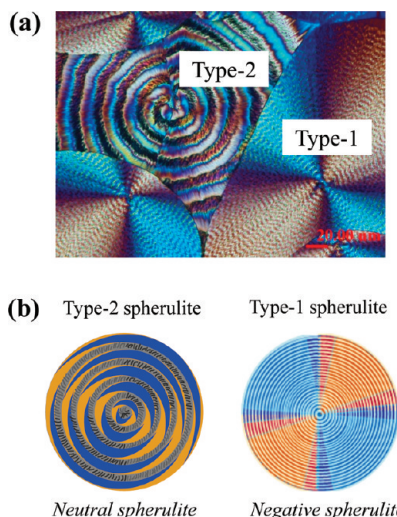


Figure 11. (a) POM graphs of Type-1 and Type-2 spherulites in PNT films melt-crystallized at $85\text{ }^\circ\text{C}$; and (b) schemes for optical birefringence patterns associated with Type-1 (negative type) and Type-2 (neutral birefringence) ring-banded spherulites.

birefringence patterns associated with these two types of ring-banded spherulites. Figure 11a shows the actual POM graphs for PNT crystallized at $T_c = 85\text{ }^\circ\text{C}$, where focus was placed on regions where both types of ring bands could be viewed. For better viewing and appreciation of difference among them, Figure 11b shows two schemes of optical birefringence and ring-band patterns (width and inter-ring spacing, etc.) of Type-1 and Type-2 ring bands crystallized at $T_c = 85\text{ }^\circ\text{C}$. Optical birefringence of Type-1 apparently differs from that of Type-2, reflecting different lamellar patterns in these two types of spherulites. As a matter of fact, they are of completely different birefringence: Type-1 ring-banded spherulite has negative-type birefringence, while Type-2 ring-banded spherulite has so large

inter-ring space and spiraling lamellar in the ridge and complicated lamellar orientation from ridge to valley that Type-2 spherulite has a neutral-type birefringence, that is, neither positive nor negative. Note that both negative Type-1 and neutral Type-2 ring-banded spherulites do not exist at separate T_c 's but coexist in PNT when crystallized at the same $T_c = 85^\circ\text{C}$. This is quite unusual that a polymer exhibits not only two types of ring bands but also both types of spherulite birefringence (negative and neutral) when crystallized at the same T_c .

4. CONCLUSIONS

PNT has been known to exhibit two interesting but entirely different types of ring-banded spherulites (labeled as Type-1 and Type-2), which were characterized to reveal nanoscale lamellar assembly patterns in the top surfaces by using AFM. One can easily note that the AFM characterization provides morphological details in the ring bands that cannot be revealed by using OM or even SEM, which require lengthy sample preparation leading to possible alteration of original fine details. These two types of ring banded spherulites were compared and analyzed in detail. First, the height profiles and orientation differences in the ridges and valley were compared. Like all other ring-banded spherulite in polymers, both types of ring-banded spherulites in PNT have similar trends with respect to temperature. With increasing T_c , (1) the vertical height variation from valley to ridge (Δz) increases either in Type-1 or in Type-2 ring-banded spherulites; however, Δz in Type-2 ring-banded spherulites is much larger than that in Type-1 ring-banded spherulites; and (2) the inter-ring period (pitch) of Type-1 ring-banded spherulites is almost the same, about 3 μm , and the width of ridge is wider than that of valley.

Further, the lamellar crystals and patterns in the ridges of these two types of ring-banded spherulites were analyzed. The lamellar crystals on the ridges of Type-1 ring-banded spherulites are irregular dough-like and remain discrete (unconnected with neighboring islands), and they are aligned in circumference to form a ring. The valley region is populated with thin needle-like crystals that are aligned in radial direction. In contrast, the crystals in ridges of Type-2 spherulites are compact, overlapped, and jammed to each other, unlike the discrete dough-like islands in ridges of Type-1 spherulites. The valley region of Type-2 spherulite at $T_c = 75^\circ\text{C}$ is populated with thin needle-like crystals that are aligned in radial direction and are similar to the crystals in valley of Type-1 spherulites. At higher T_c (85°C), the general morphology of Type-2 spherulites retains some similarity but also exhibits some distinct difference from that crystallized at lower T_c (75°C). The crystals in ridges of Type-2 spherulites are also compact, overlapped, and jammed to each other; in addition, they are elongated to a longer lenticular-shape and oriented to $+45^\circ$ to the radial direction. The valley region of Type-2 spherulite at $T_c = 85^\circ\text{C}$ is populated with thin needle-like crystals that are aligned in -30° from radial direction.

The crystal packing on the ridges and valley of these two types of ring-banded was compared using high-magnification AFM phase imaging. Interestingly, there exists a transition zone in going from the ridge and valley regions in the Type-2 ring-banded spherulites crystallized at $T_c = 75-85^\circ\text{C}$; the crystals on the transition zone change gradually in sizes and orientation from those in the ridge to valley. On the other hand, Type-1 ring-banded spherulite does not have this kind of transition zone, meaning that crystals in the ridges abruptly submerge into

valley in Type-1 ring-banded spherulites. Type-1 ring-banded spherulite remains a negative type in the birefringence imposed with ring-bands when crystallized at any T_c . By contrast, for Type-2 ring-banded spherulites crystallized at an even higher $T_c = 85^\circ\text{C}$, there exists a broader transition zone between the valley and ridge regions. The different lamellar orientation in the ridge and valley region and the broad transition zones between them altogether lead to a neutral birefringence in Type-2 ring-banded spherulites at $T_c = 85^\circ\text{C}$.

■ AUTHOR INFORMATION

Corresponding Author

*Tel.: +886 6 275-7575 ext. 62670. Fax: +886 6 234-4496. E-mail: emwoo@mail.ncku.edu.tw.

Notes

The authors declare no competing financial interest.

■ ACKNOWLEDGMENTS

This work has been financially supported by a basic research grant (NSC-97-2221-E-006-034-MY3) for three consecutive years from Taiwan's National Science Council (NSC), for which we express our gratitude.

■ REFERENCES

- (1) Chen, Y. F.; Woo, E. M. *Macromol. Rapid Commun.* **2009**, *30*, 1911–1916.
- (2) Woo, E. M.; Nurkhamidah, S.; Chen, Y. F. *Phys. Chem. Chem. Phys.* **2011**, *13*, 17841–17851.
- (3) Kyu, T.; Chiu, H. W.; Guenther, A. J.; Okaba, Y.; Saito, H.; Inoue, T. *Phys. Rev. Lett.* **1999**, *83*, 2749–2752.
- (4) Schultz, J. M. *Polymer* **2003**, *44*, 433–441.
- (5) Toda, A.; Arita, T.; Hikosaka, M. *Polymer* **2001**, *42*, 2223–2233.
- (6) Bassett, D. C. *J. Macromol. Sci., Part B: Phys.* **2003**, *42*, 227–256.
- (7) Keith, H. D.; Padden, F. J., Jr. *Polymer* **1984**, *25*, 28–42.
- (8) Murayama, E. *Polym. Prepr. Jpn.* **2002**, *51*, 460.
- (9) Sasaki, S.; Sakaki, Y.; Takahara, A.; Kajiyama, T. *Polymer* **2002**, *43*, 3441–3446.
- (10) Ivanov, D. A.; Jonas, A. M. *Macromolecules* **1998**, *31*, 4546–4550.
- (11) Li, L.; Chan, C. M.; Li, J. X.; Ng, K. M.; Yeung, K. L.; Weng, L. T. *Macromolecules* **1999**, *32*, 8240–8242.
- (12) Chen, J.; Yang, D. *Macromol. Rapid Commun.* **2004**, *25*, 1425–1428.
- (13) Markey, L.; Janimak, J. J.; Stevens, G. C. *Polymer* **2001**, *42*, 6221–6230.
- (14) Wang, Y.; Ge, S.; Rafailovich, M.; Sokolov, J.; Zou, Y.; Ade, H.; Lüning, J.; Lustiger, A.; Maron, G. *Macromolecules* **2004**, *37*, 3319–3327.
- (15) Briber, R. M.; Khouri, F. J. *Polym. Sci., Part B: Polym. Phys.* **1993**, *31*, 1253–1272.
- (16) Xu, J.; Guo, B. H.; Zhang, Z. M.; Zhou, J. J.; Jiang, Y.; Yan, S.; Li, L.; Wu, Q.; Chen, G. Q.; Schultz, J. M. *Macromolecules* **2004**, *37*, 4118–4123.
- (17) Guerra, G.; Vitagliano, V. M.; De Rosa, C.; Petraccone, V.; Corradini, P. *Macromolecules* **1990**, *23*, 1539–1544.
- (18) Sun, Y. S.; Woo, E. M. *Macromolecules* **1999**, *32*, 7836–7844.
- (19) Woo, E. M.; Sun, Y. S.; Yang, C. P. *Prog. Polym. Sci.* **2001**, *26*, 945–983.
- (20) Brückner, S.; Meille, S. V.; Petraccone, V.; Pirozzi, B. *Prog. Polym. Sci.* **1991**, *16*, 361–404.
- (21) Lotz, B. *Polymer* **1998**, *39*, 4561–4567.
- (22) Geil, P. H. *Polymer Single Crystals*; Interscience: New York, 1963.
- (23) Keller, A.; Warner, M.; Windle, A. H., Eds. *Self-Order and Forms in Polymeric Materials*; Chapman and Hall: London, 1995.

(24) Frömsdorf, A.; Woo, E. M.; Lee, L.-T.; Chen, Y. F.; Förster, S. *Macromol. Rapid Commun.* **2008**, *29*, 1322–1328.